Allele-Selective Inhibition of Mutant *Huntingtin* Expression with Antisense Oligonucleotides Targeting the Expanded CAG Repeat[†]

Keith T. Gagnon,[‡] Hannah M. Pendergraff,[‡] Glen F. Deleavey,[§] Eric E. Swayze,[‖] Pierre Potier,[⊥] John Randolph,[#] Eric B. Roesch,[#] Jyoti Chattopadhyaya,[▽] Masad J. Damha,[§] C. Frank Bennett,[‖] Christophe Montaillier,[⊥] Marc Lemaitre,[#,○] and David R. Corey*,[‡]

[‡]*Departments of Pharmacology and Biochemistry, UT Southwestern Medical Center, ND8.136B, Dallas, Texas 75390-9041, United States,* [§]*Department of Chemistry, McGill University, Montreal, Quebec H3A 2K6, Canada,* [‖]*Isis Pharmaceuticals, 1896 Rutherford Road, Carlsbad, California 92008, United States,* [⊥]*SIGMA Custom Products, Genopole Campus 1, 5 Rue Desbruères, 91030 Evry Cedex, France,* [#]*Glen Research Corporation, 22825 Davis Drive, Sterling, Virginia 20164, United States, and* [▽]*Department of Bioorganic Chemistry, Uppsala University, Biomedical Center, Box 581, S-751 23 Uppsala, Sweden.* [○]*Current Address: Girindus America Inc., 8560 Reading Road. Cincinnati, Ohio 45215, United States.*

ABSTRACT: Huntington's disease (HD) is a currently incurable neurodegenerative disease caused by the expansion of a CAG trinucleotide repeat within the *huntingtin* (*HTT*) gene. Therapeutic approaches include selectively inhibiting the expression of the mutated *HTT* allele while conserving function of the normal allele. We have evaluated a series of antisense oligonucleotides (ASOs) targeted to the expanded CAG repeat within *HTT* mRNA for their ability to selectively inhibit expression of mutant HTT protein. Several ASOs incorporating a variety of modifications, including bridged nucleic acids and phosphorothioate internucleotide linkages, exhibited allele-selective silencing in patient-derived fibroblasts. Allele-selective ASOs did not affect the expression of other CAG repeat-containing genes and selectivity was observed in cell lines containing minimal CAG repeat lengths representative of most HD patients. Allele-selective ASOs left *HTT* mRNA intact and did not support ribonuclease H activity in vitro. We observed cooperative binding of multiple ASO molecules to CAG repeat-containing *HTT* mRNA transcripts in vitro. These results are consistent with a mechanism involving inhibition at the level of translation. ASOs targeted to the CAG repeat of *HTT* provide a starting point for the development of oligonucleotide-based therapeutics that can inhibit gene expression with allelic discrimination in patients with HD.

Expansion of unstable trinucleotide repeats is responsible for at least 16 inherited neurological disorders (*1*). Although Huntington's disease is one of the most well-known trinucleotide repeat diseases, it remains incurable and insufficiently understood. HD[1] has a prevalence of 1 in 10000−15000 in populations of European descent and is characterized by adult onset and progressive neurodegeneration (*2*). Symptoms include chorea, dystonia, and cognitive or psychiatric disturbances. These symptoms gradually worsen until death 10−20 years after disease onset (*2, 3*).

The expansion of a CAG repeat in exon 1 of the *Huntingtin* (*HTT*) gene leads to the autosomal dominant disease (*3, 4*). Expansion beyond 36 repeats is associated with HD, and full disease penetrance is observed for repeat lengths > 41 (*5−8*). The CAG repeat encodes a poly glutamine (poly-Q) tract at the N-terminus of the HTT protein and repeat length is inversely correlated with age at disease onset in patients with HD (*2, 7*).

The expanded poly-Q tract in HTT confers a gain of function, namely oligomerization of mutant HTT poly-Q fragments, disables efficient protein degradation pathways, and may interfere with normal protein functions (*2, 4, 9, 10*). Aggregation of poly-Q containing HTT fragments eventually induces the formation of plaques in the brains of patients with HD (*11*). Cells in the central nervous system and brain are sensitive to these changes, especially the corticostriatal neurons of the striatum, which suffer the greatest degeneration (*2, 9, 11*).

Therapeutic options for HD include small molecule drugs like haloperidol, tetrabenazine, clonazepam, fluoxitine, and sertraline that are designed to control the phenotypic manifestations of the disease (*12−15*). While these drugs can improve quality of life for patients with HD, they are not expected to significantly reverse or alter disease progression or increase life expectancy nor do they address the underlying molecular mechanisms of the disease (*12*).

HTT is a large protein (348 kDa) predicted to interact with over 180 proteins and has been reported to influence several pathways, including transcription, apoptosis, mitochondrial function and energy metabolism, tumor suppression, vesicular and neurotransmitter release, and axonal transport (*4, 16−19*). Drug development has targeted several cellular pathways, including coenzyme Q_{10} analogues for mitochondrial dysfunction and farnesyltransferase inhibitors to upregulate autophagy (*20, 21*). Therapeutic intervention is complicated because targeting a single pathway may only partially alleviate the disease.

*To whom correspondence should be addressed. Phone: 214-645-6153. Fax: 214-645-6067. E-mail: david.corey@utsouthwestern.edu.

[1]Abbreviations: *HTT, Huntingtin*; ASO, antisense oligonucleotide; HD, Huntington's disease; SNP, single nucleotide polymorphism; siRNA, small interfering RNA; LNA, locked nucleic acid; BNA, bridged nucleic acid; DSC, differential scanning calorimetry; UV, ultraviolet; qPCR, quantitative polymerase chain reaction; EMSA, electrophoretic mobility shift assay.

Published on Web 10/28/2010

One direct route to treating HD would be reduction or elimination of the causative agent, the mutant protein itself. *HTT* is an essential gene that is required in embryogenesis, neurogenesis, and normal adult function (*22*, *23*), and evidence suggests that 30−40% expression of wild-type *HTT* is necessary to support normal development and function (*21*, *23*−*25*). Thus, to maintain sufficient levels of normal HTT protein, and because almost all patients have one normal and one mutant *HTT* gene (*4*, *7*), potential therapeutic strategies include reducing expression of the mutant *HTT* allele (*26*).

One strategy for allele-selective inhibition of *HTT* expression is development of small interfering RNAs (siRNAs) that target single-nucleotide polymorphisms (SNPs) or deletion polymorphisms (*27*−*31*). Recent reports suggest that a small number of siRNAs targeting different SNP sites could potentially treat >75% of patients with HD (*31*, *32*). However, the need to develop a collection of related drugs would complicate clinical development. Thus, while SNP-targeted siRNAs are an important approach for developing selective agents, there remains a need for alternate strategies.

Single-stranded complementary oligomers containing peptide nucleic acid (PNA) or locked nucleic acid (LNA) can selectively inhibit expression of the mutant *HTT* allele (*33*−*35*). A similar antisense approach has been described recently in which complementary morpholino oligomers block the binding of muscleblind like 1 (MBNL-1) to expanded CUG repeats and affect the pathogenesis of myotonic dystrophy (*36*). Antisense oligonucleotides (ASOs) contain a single nucleic acid strand that can be heavily modified to enhance stability, target binding, and biodistribution. ASOs have been extensively investigated in the clinic as a therapeutic approach (*26*, *37*, *38*), and promising phase III data has been recently presented for Mipomersen, an ASO that reduces expression of apolipoprotein B (*39*−*41*).

Here we test a broad spectrum of modified ASOs targeted to the CAG repeat within *HTT* mRNA and identify several that achieve allele-selective inhibition. ASOs targeting expanded trinucleotide repeat regions of mRNA may represent a route to allele-selective therapeutics for treatment of HD and other repeat expansion diseases.

MATERIALS AND METHODS

Oligonucleotides. ASOs were synthesized and purified by Isis Pharmaceuticals, Sigma Custom Products, Glen Research Corporation, and the Damha laboratory. Unmodified DNA and RNA were purchased from Integrated DNA Technologies, Inc.

Thermal Denaturation by UV Melt Analysis. Thermal denaturation analysis of ASOs or ASO:RNA duplexes was carried out using a CARY Varian model 3 UV−vis spectrophotometer. Absorbance was monitored at 260 nm in a 1 cm quartz cuvette. ASO (0.8 μM) or ASO annealed to complementary RNA (0.8 μM) in 1× Dulbecco's phosphate-buffered saline (Sigma Aldrich) was annealed and melted three times from 18 to 99 °C at a ramp rate of 2 °C/min. To evaluate the concentration dependence of T_m, 0.1 cm quartz cuvettes were used with variable concentrations of oligonucleotide ranging from 0.5 to 50.0 μM. Absorbance was collected at one reading per 1 °C. T_m was calculated using CARY WinUV Thermal Application software using a baseline fitting method.

Thermal Denaturation by Differential Scanning Calorimetry. Differential scanning calorimetry (DSC) was performed on a MicroCal VP-DSC capillary cell microcalorimeter. ASOs or ASO:RNA duplexes at 10 or 20 μM in degassed 1× Dulbecco's phosphate-buffered saline (Sigma Aldrich) were first heated to 95 °C for 5 min and then cooled to room temperature on the benchtop to allow duplex annealing. Samples were scanned under pressure from 35 to 125 °C at a scan rate of 90 °C/h with 2 rescans. The peak change in heat capacity (C_p) was determined using Origin 7.0 with DSC Data Analysis (MicroCal) software. The temperature corresponding to the maximum peak in C_p of the ASO or ASO:RNA duplex was taken as the T_m. Replicate scans were used to calculate the average T_m and standard deviation. Origin 7.0 with DSC Data Analysis software was also used to fit DSC scans to a two-state unfolding model and calculate enthalpy.

Cell Culture and Transfection. Patient-derived fibroblast cell lines GM04281 (69 CAG repeat mutant allele), GM04717 (41 CAG repeat mutant allele), and GM04719 (44 CAG repeat mutant allele) were obtained from the Coriell Institute. Cells were maintained at 37 °C and 5% CO2 in MEM (Sigma) supplemented with 10% FBS (Sigma) and 0.5% MEM nonessential amino acids (Sigma). Cells were plated in 6-well dishes at 60000 cells/well in supplemented MEM 2 days before transfection. Stock solutions of modified ASOs were heated at 65 °C for 5 min prior to use to dissolve any aggregation. Modified ASOs were transfected into cells using RNAiMAX (Invitrogen) according to the manufacturer's instructions. The appropriate amount of lipid (2 μL for 125 pmol ASO) was added to OptiMEM containing oligonucleotides, and the oligonucleotide−lipid mixture (250 μL) was incubated for 20 min. OptiMEM was added to the mixture to a final volume of 1.25 mL and then added to cells. Media was exchanged 1 day after transfection with fresh supplemented MEM. Cells were washed with phosphate-buffered saline and harvested 4 days after transfection for protein analysis or at 3 days for RNA analysis.

Western Blot Analysis. Cells were harvested with trypsin-EDTA solution (Invitrogen) and lysed. The protein concentration in each sample was quantified with micro bicinchoninic acid (micro-BCA) assay (Thermo Scientific). SDS-PAGE (separating gel: 5% acrylamide-bisacrylamide [50:1], 450 mM Tris-acetate pH 8.8; stacking gel: 4% acrylamide-bisacrylamide [50:1], 150 mM Tris-acetate pH 6.8) was used to separate wild-type and mutant HTT proteins. Gels were run at 30 mA per gel for 5 h in Novex Tris-acetate SDS running buffer (Invitrogen). For separation of *HTT* variants containing shorter CAG repeats, gels were run for 6−7 h. The electrophoresis apparatus was placed in a 15 °C water bath to prevent overheating. In parallel with analysis for *HTT* expression, samples were analyzed for β-actin expression by SDS-PAGE (7.5% acrylamide precast gels; Bio-Rad) to ensure even loading of protein in all lanes. These gels were run at 80 V for 15 min followed by 100 V for 1 h in 1× TGS buffer (Bio-Rad).

After electrophoresis, proteins were transferred to membrane (Hybond-C Extra; GE Healthcare Bio-Sciences). Primary antibodies specific for HTT (MAB2166, Chemicon) and β-actin (Sigma) protein were obtained and used at 1:10000 dilutions. HRP conjugate antimouse secondary antibody (1:10000, Jackson ImmunoResearch Laboratories) was used for visualizing proteins using SuperSignal West Pico Chemiluminescent Substrate (Thermo Scientific). Detection of TBP and FOXP2 was performed similar to that of a previous description (*33*). Briefly, samples were run on 7.5% precast gels (Bio-Rad), transferred to membrane and probed with a 1:5000 or 1:1000 dilution of anti-TBP (Sigma) or anti-FOXP2 (Abcam), respectively, at 4 °C overnight. HRP conjugate antimouse or antirabbit (1:5000)

(Jackson ImmunoResearch Laboratories) was used to visualize TBP and FOXP2, respectively, with SuperSignal West Pico Chemiluminescent Substrate (Thermo Scientific). Protein bands were quantified from autoradiographs using ImageJ software. Percentage of inhibition was calculated as a relative value to control samples.

Each data plot from dose response experiments for inhibition of *HTT* was fit to the following model equation: $y = 100(1 - x^m/(n^m + x^m))$ using Prism 4.0 (GraphPad), where y is percent expression of HTT protein and x is concentration of ASO. Both m and n are fitting parameters, where n is taken as the IC_{50} value. The IC_{50} values were calculated from individual dose responses fit to the above equation and then reported as the mean and standard error of the mean of three or more biological replicates.

Quantitative PCR (qPCR). Total RNA from fibroblast cells was extracted using TRIzol (Invitrogen) 3 days after transfection. Two μg of RNA was treated with 2 units of DNase I (Worthington Biochemical Corp.) for 10 min at 25 °C. RNA was reverse transcribed using a High Capacity cDNA Reverse Transcription Kit (Applied Biosystems) according to the manufacturer's protocol. Quantitative PCR was performed on a BioRad CFX96 real time system using iTaq SYBR Green Supermix with ROX (Bio-Rad). Data were normalized relative to levels of GAPDH mRNA. Primers specific for the *HTT* exon 64−65 boundary were used: forward primer, 5′-CGACAGCG-AGTCAGTGAATG-3′; reverse primer, 5′-ACCACTCTGGC-TTCACAAGG-3′. Primers specific for GAPDH were obtained from Applied Biosystems. Experiments were performed in biological triplicate and error reported as standard deviation.

Cloning and in Vitro Transcription of 5′ Truncated HTT mRNA Transcripts. Sequence corresponding to the 5′ end of *HTT* mRNA was cloned from GM04281 fibroblasts. Total RNA was extracted with TRIzol (Invitrogen), DNase I-treated and reverse transcribed with random primers using a High Capacity cDNA Reverse Transcription Kit (Applied Biosystems). Complementary DNA was amplified by PCR with HotStarTaq DNA Polymerase (Qiagen) following the manufacturer's protocol and using the following primers: forward primer, 5′-ATGGCGAC-CCTGGAAAAG-3′; reverse primer, 5′-GGCTGAGGAAGCT-GAGGGAG-3′. PCR products were gel-purified and cloned into the pCR 4-TOPO plasmid using the TOPO-TA Cloning Kit (Invitrogen) following the manufacturer's recommended protocol. The cloning of the 5′ cDNA sequence of *HTT* mRNA was verified by sequencing.

Plasmids were linearized with *Pme* I restriction enzyme and used for the production of REP69 or REP17 RNAs by in vitro runoff transcription using an Ampliscribe T7-Flash Transcription Kit (Epicentre). RNAs were extracted with pH 4.3 phenol and 24:1 chloroform:isoamyl alcohol. One volume of gel purification buffer (1× TBE, 90% formamide) was added and the RNA solution boiled for 5 min. RNA samples were resolved on 6% denaturing polyacrylamide gels (7 M urea, 1× TBE) and the bands visualized by lightly staining with methylene blue before being cut out. RNA was extracted by crush and soak elution with RNA elution buffer (20 mM Tris, pH 7.4, 5 mM EDTA, 0.3 M sodium acetate, 0.1% SDS) then precipated with two volumes of ethanol.

Electrophoretic Mobility Shift Assays (EMSA). Twenty pmols of REP69 or REP17 RNA was dephosphorylated in a 40 μL reaction containing 10 U of calf intestinal phosphatase (CIP) (New England Biolabs), 1× CIP buffer, and 20 U of SUPERase-In RNase Inhibitor (Ambion) for 15 min at 37 °C

and then 15 min at 55 °C. RNA was extracted with pH 4.3 phenol and 24:1 chloroform:isoamyl alcohol then precipitated with 0.3 M sodium acetate and 70% ethanol. CIP-treated RNA was 5′-end labeled in a 25 μL reaction containing 20 U of T4 polynucleotide kinase (T4 PNK) (New England Biolabs), 1× PNK buffer, 20 U of SUPERase-In, and 3 μL of [γ]-^{32}P ATP (7000 Ci/mmol) (MP Biomedicals) and then incubated at 37 °C for 1.5 h. Radiolabeled RNA was extracted with pH 4.3 phenol and 24:1 chloroform:isoamyl alcohol. RNA was gel-purified as described above for unlabeled RNA, except that the RNA bands were visualized by a phosphorimager and radioactivity quantified by liquid scintillation counting.

To evaluate ASO binding to structured REP17 and REP69 RNAs, electrophoretic mobility shift assays (EMSA) were performed. Radiolabeled RNA was refolded in 1× EMSA buffer (25 mM Phosphate buffer, pH 7.0, 0.2 mM EDTA, 0.15 M NaCl, 1 mM MgCl$_2$) by heating to 98 °C then cooling to 25 °C at a rate of 0.1 °C/s. Increasing concentrations of ASO were mixed with the refolded RNA (80 fmols, 20000 cpm) in a 10 μL reaction containing 1× EMSA buffer, 5 U SUPERase-In, and 10 μg yeast tRNA and incubated at 37 °C for 15 min. Reactions were moved to room temperature, 2.5 μL of phosphate buffer dye (0.25 M phosphate buffer, pH 7.0, 50% glycerol, 0.02% bromophenol blue, 0.02% xylene cyanol) added, and then loaded onto a 0.75 mm thick native polyacrylamide gel (25 mM phosphate, pH 7.0, 6% 19:1 acrylamide:bisacrylamide, 2% glycerol). Gels were run with cooling for 5−6 h at 150 V then dried to 3 M Whatman paper and exposed to phosphorimager cassettes for visualization.

Shifted RNA was quantified with ImageJ software and fit to a Hill equation: $y = (x^n)/(K_d{}^n + x^n)$ using Prism 4.0 (GraphPad), where y is the fraction of RNA shifted and x is the concentration of ASO. Both K_d and n are fitting parameters, where K_d is taken as the dissociation constant and n is the Hill coefficient.

In Vitro RNase H Activity Assay. Radiolabeled REP69 RNA (0.1 pmol, 20,000 cpm) was incubated with ASO (10 pmol) and 1 mg/mL yeast tRNA in 1× EMSA buffer in a 9.5 μL reaction for 5 min at 37 °C. RNase H1 enzyme from *Escherichia coli* (1 U) (Invitrogen) was added for a final reaction volume of 10 μL and incubated for 10 min at 37 °C. Reactions were stopped by the addition of 9 volumes of 2% LiClO$_4$ in acetone. Reactions were spun down, pellets washed with acetone and resuspended in gel purification buffer, boiled for 5 min, and then resolved on 5% denaturing polyacrylamide gels supplemented with 2% glycerol. Gels were run at 250 V for 2.5 h, dried to 3 M Whatman paper, and visualized by a phosphorimager.

RESULTS

Strategy for Designing and Testing Modified Oligonucleotides. We designed modified antisense oligonucleotides (ASOs) to optimize allele-selective inhibition and gain further insights into mechanism. Our lead compound was LNA(T) (*33, 34*). LNA(T) is a 19 nucleotide long oligonucleotide consisting of repeating GCT sequence with 3′ and 5′ terminal guanines. LNA(T) targets the CAG repeat sequence in exon 1 of *HTT* mRNA and contains deoxyribonucleic acid (DNA) nucleotides mixed with LNA nucleotides at every third base, in this case at every thymine residue (Figure 1A). Thermodynamic effects of the LNA are largely propagated to the nearest neighboring 5′ and 3′ nucleotides (*42*). Thus, for a G-C rich 19 base oligonucleotide, this configuration is preferred because it produces high affinity binding and minimizes manufacturing costs.
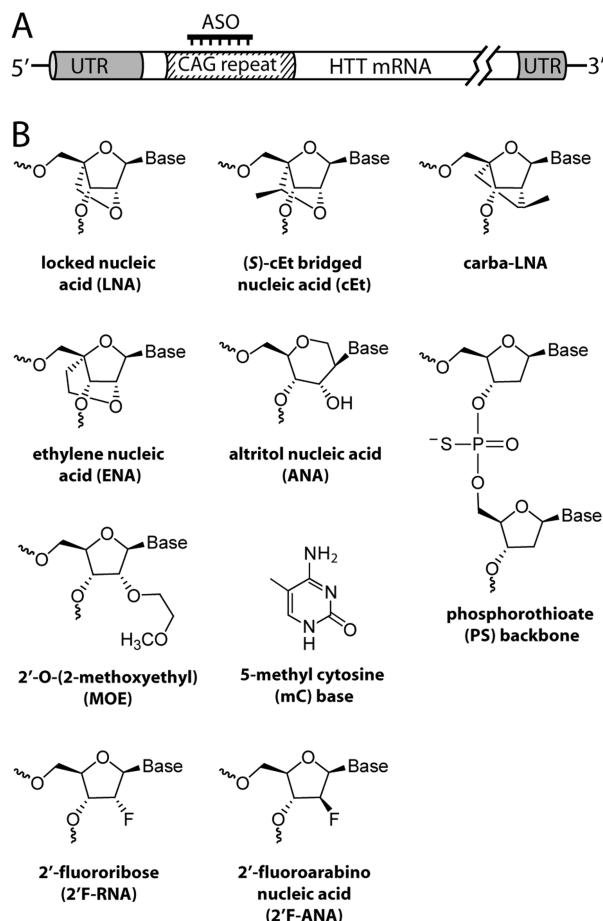
FIGURE 1: Strategy for targeting the expanded CAG repeat region of mutant *HTT* mRNA to elicit allele-selective inhibition. (A) Schematic of the *HTT* mRNA and the CAG repeat region that is targeted with complementary CTG-repeat ASOs. UTR, untranslated region. (B) Chemically modified base, backbone, and nucleosides incorporated into ASOs tested for allele-selective inhibition of *HTT* expression.

LNA is a member of a class of modifications called bridged nucleic acid (BNA) (*43, 44*). BNA is characterized by a covalent linkage that locks the conformation of the ribose ring in a C3′-*endo* (northern) sugar pucker. For LNA, the bridge is composed of a methylene between the 2′-*O* and the 4′-*C* positions. LNA enhances backbone preorganization and base stacking to increase hybridization and thermal stability (Figure 1B) (*43–46*).

Three other BNA modifications were tested: 2′-*O*,4′-*C*-ethylene-bridged nucleic acid (ENA), 2′,4′-constrained ethyl nucleic acid called *S*-cEt (cEt), and 2′-4′-carbocyclic LNA (carba-LNA) (Figure 1B). These modifications enhance the affinity of binding and protect the oligonucleotide against nuclease digestion. ENA provides a more flexible bridge than LNA (*47, 48*). The cEt modification has been shown to possess a favorable toxicity profile in animals (*49, 50*). Carba-LNA retains LNA-like properties but is chemically unique in that it lacks oxygen on the 2′ carbon (*51*). We also tested altritol nucleic acid (ANA) consisting of a six-membered D-altritol sugar with a nucleobase attached at the 2′-position and a hydroxyl group at the 3′-position. ANA rigidifies the base conformation, improves thermal stability, and reduces digestion by nuclease (*52*). A practical advantage for all BNA nucleotides is that they can be substituted within RNA or DNA oligomers, simplifying synthesis and allowing the properties of the parent oligomer to be fine-tuned for specific applications.

We also examined substitution at the 2′ position of the ribose with fluorine in either stereoisomer orientation (2′F-RNA or 2′F-ANA) or 2′-*O*-(2-methoxyethyl) (MOE) (Figure 1B). These 2′ modifications improve nucleic acid hybridization and duplex stability (*53–55*). 2′F-ANA is known to support RNase H cleavage with efficiencies that vary depending on the location of substitution (*55, 56*). Some oligomers were "gapmer" designs that incorporate modifications near the termini of the oligonucleotide while leaving the central portion as native DNA or containing RNase H-compatible substitutions (*57*). The RNase H enzyme recognizes the ASO:RNA duplex and catalytically cleaves the RNA substrate.

Oligonucleotides consisting of repeating GCT sequence are partially self-complementary and have potential to form hairpin structures (*58, 59*). Hairpin formation might affect recognition of the mRNA target. To investigate the stability of ASO self-structures and ASO:RNA duplexes, we used UV melt analysis and differential scanning calorimetry (DSC) (Figure S1 of the Supporting Information). DSC was useful for measuring very high T_m values because it can scan samples under pressure at temperatures up to 130 °C. The temperature corresponding to a maximum change in heat capacity (C_p) of the ASO:RNA duplex can be taken as the T_m (*60, 61*).

Selective Inhibition of Mutant HTT Expression with LNA-Modified ASOs. LNAs were evaluated in patient-derived GM04281 fibroblasts (Figures 2, S2 and S3 of the Supporting Information). GM04281 cells harbor a normal *HTT* allele of 17 CAG repeats and a mutant allele with 69 CAG repeats and we have used this cell line previously to investigate allele-selective inhibition of *HTT* (*33–35*).

We tested a variety of LNAs that differed in length, position of LNA substitution, and register of the sequence relative to the target triplet repeat. Four ASOs, LNA(T), LNA(G), LNA(T)+2, and LNA(T)22, inhibited *HTT* expression in an allele-selective fashion. Quantification of Western blots after dose response treatments revealed potencies ranging from IC_{50} values of 27–40 nM and selectivities of inhibition for mutant versus wild-type *HTT* by as much as > 3.7 fold (Figure 2A).

LNA-gap, which contains a central DNA portion capable of recruiting RNase H, inhibited *HTT* expression with lower selectivity (2.1-fold). We noted, however, that the introduction of LNA-gap into cells caused a moderate amount of cell death (Figure S4 of the Supporting Information). One explanation is that the ability to recruit RNase H might cause greater inhibition of other genes that contain CAG repeats because gapmer designs would cause catalytic degradation of RNA targets. Over 300 exonic sequences in humans are predicted to contain six or more repeated CAG units (*62*). Inhibition of both *HTT* alleles is not the cause of toxicity because siHdh1, an siRNA inhibiting both alleles and directed against sequences downstream of the repeat region (*63*) (see Figure 6A), showed no toxicity.

Although only four LNA-modified ASOs exhibited clear allele-selective inhibition, all 19 and 22 nucleotide LNAs hybridized to CAG repeat RNA with comparably high T_m values. These data indicate that the potential for strong hybridization may be necessary but not sufficient for allele-selectivity (Figure 2A). Loss of inhibition by shortening of the benchmark ASO [LNA(T)16 or LNA(T)13] correlated with reduced T_m values for hybridization to a complementary RNA. Although substitution of the T or G bases resulted in inhibitory and allele-selective ASOs, modification of cytosine positions with LNA did not yield inhibitory oligonucleotides. Interestingly, these same

A

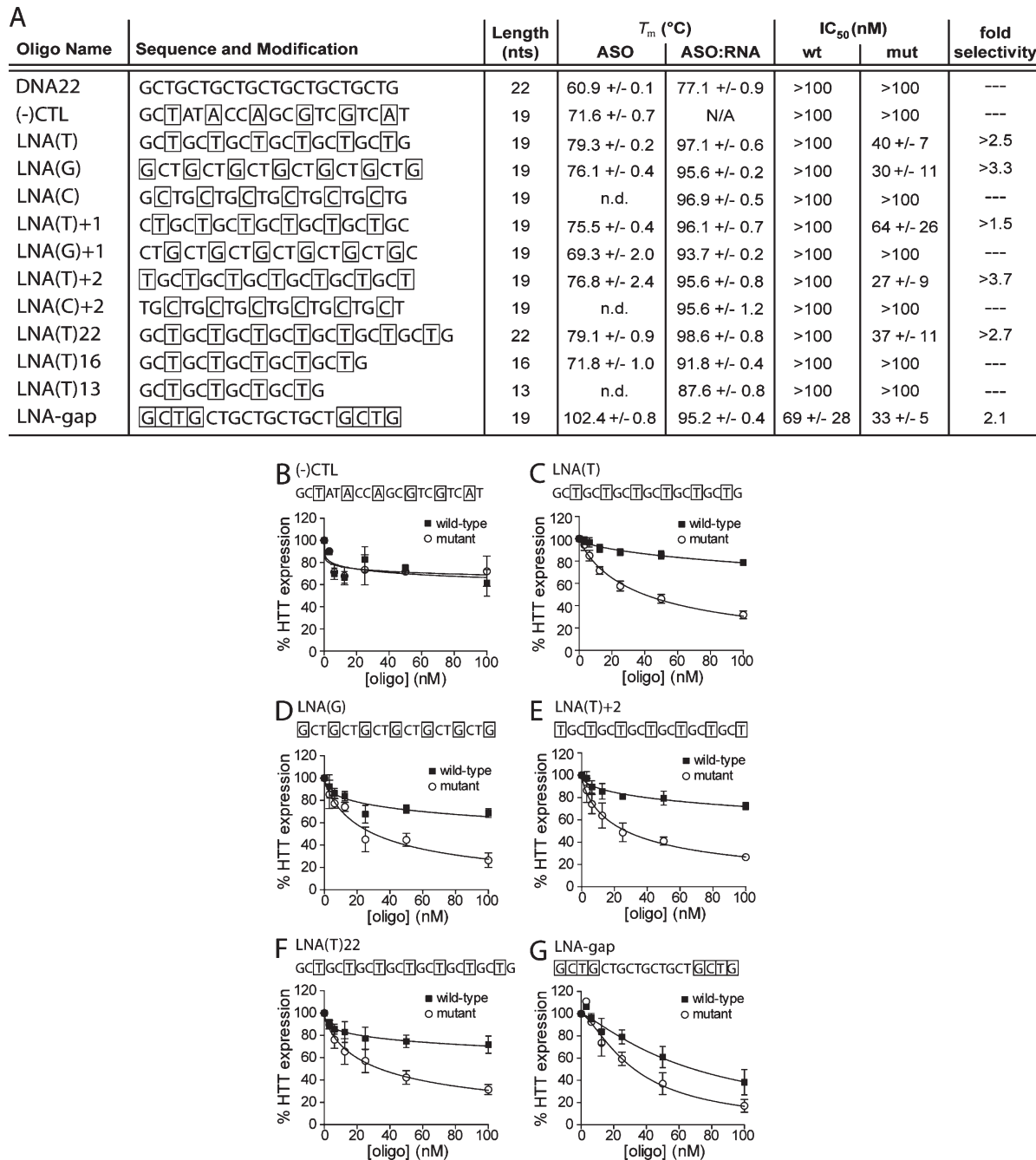| Oligo Name	Sequence and Modification	Length (nts)	T_m (°C) ASO	T_m (°C) ASO:RNA	IC$_{50}$ (nM) wt	IC$_{50}$ (nM) mut	fold selectivity
DNA22	GCTGCTGCTGCTGCTGCTGCTG	22	60.9 +/- 0.1	77.1 +/- 0.9	>100	>100	---
(-)CTL	GC[T]AT[A]CC[A]GC[G]TC[G]TC[A]T	19	71.6 +/- 0.7	N/A	>100	>100	---
LNA(T)	GC[T]GC[T]GC[T]GC[T]GC[T]GC[T]G	19	79.3 +/- 0.2	97.1 +/- 0.6	>100	40 +/- 7	>2.5
LNA(G)	[G]CT[G]CT[G]CT[G]CT[G]CT[G]CT[G]	19	76.1 +/- 0.4	95.6 +/- 0.2	>100	30 +/- 11	>3.3
LNA(C)	G[C]TG[C]TG[C]TG[C]TG[C]TG[C]TG	19	n.d.	96.9 +/- 0.5	>100	>100	---
LNA(T)+1	C[T]GC[T]GC[T]GC[T]GC[T]GC[T]GC	19	75.5 +/- 0.4	96.1 +/- 0.7	>100	64 +/- 26	>1.5
LNA(G)+1	CT[G]CT[G]CT[G]CT[G]CT[G]CT[G]C	19	69.3 +/- 2.0	93.7 +/- 0.2	>100	>100	---
LNA(T)+2	[T]GC[T]GC[T]GC[T]GC[T]GC[T]GC[T]	19	76.8 +/- 2.4	95.6 +/- 0.8	>100	27 +/- 9	>3.7
LNA(C)+2	TG[C]TG[C]TG[C]TG[C]TG[C]TG[C]T	19	n.d.	95.6 +/- 1.2	>100	>100	---
LNA(T)22	GC[T]GC[T]GC[T]GC[T]GC[T]GC[T]GC[T]G	22	79.1 +/- 0.9	98.6 +/- 0.8	>100	37 +/- 11	>2.7
LNA(T)16	GC[T]GC[T]GC[T]GC[T]GC[T]G	16	71.8 +/- 1.0	91.8 +/- 0.4	>100	>100	---
LNA(T)13	GC[T]GC[T]GC[T]GC[T]G	13	n.d.	87.6 +/- 0.8	>100	>100	---
LNA-gap	[G][C][T][G]CTGCTGCTGCT[G][C][T][G]	19	102.4 +/- 0.8	95.2 +/- 0.4	69 +/- 28	33 +/- 5	2.1

FIGURE 2: Selective inhibition of mutant *HTT* expression is observed with LNA-modified ASOs of varying sequence, length, or modification configuration. (A) Properties of LNA-modified ASOs that are complementary to the *HTT* mRNA CAG repeat sequence. ASO, antisense oligonucleotide alone; ASO:RNA, antisense oligonucleotide duplexed with complementary RNA. DNA22 is an unmodified DNA oligo and (−)CTL is a scrambled sequence containing LNA at every third base. Bases enclosed by boxes indicate LNA modification position. T_m values were experimentally determined by UV melt analysis for ASOs and differential scanning calorimetry (DSC) for ASO:RNA duplexes. Error is standard deviation. IC$_{50}$ values are calculated from Western blot quantification. Values are reported in mean ± standard error of the mean (SEM). N/A, not applicable; nd, not determined due to insufficient cooperativity. (B−G) HTT protein expression in patient-derived fibroblast cells containing 69 CAG repeats in the mutant allele (GM04281) in response to increasing doses of control and inhibitory ASOs. Quantification and a nonlinear fit of *HTT* expression levels from multiple dose responses are plotted. Sequence and modification configuration are indicated above the graph. Error bars are SEM.

two oligonucleotides, LNA(C) and LNA(C)+2, were observed to have poor cooperative melting and low hyperchromicity, which prevented accurate T_m determination. Poor cooperativity during thermal denaturation is indicative of low secondary structure or a population of conformationally irregular, nonhomogeneous structures, such as aggregates (64, 65), suggesting a role for the degree and nature of self-interactions in effective inhibition with LNA-modified ASOs that target CAG repeats.

Effect of Other Bridged Nucleic Acid (BNA) and 2′ Sugar Modifications on Allele-Selective Inhibition. To broaden the base of compounds available for development, obtain structure−activity relationships for allele selective inhibition, and gain additional mechanistic insights, we tested oligomers containing other chemically modified nucleotides. We evaluated inhibition of *HTT* expression with oligonucleotides containing ENA, cET, carba-LNA, 2′F-RNA, 2′F-ANA, or
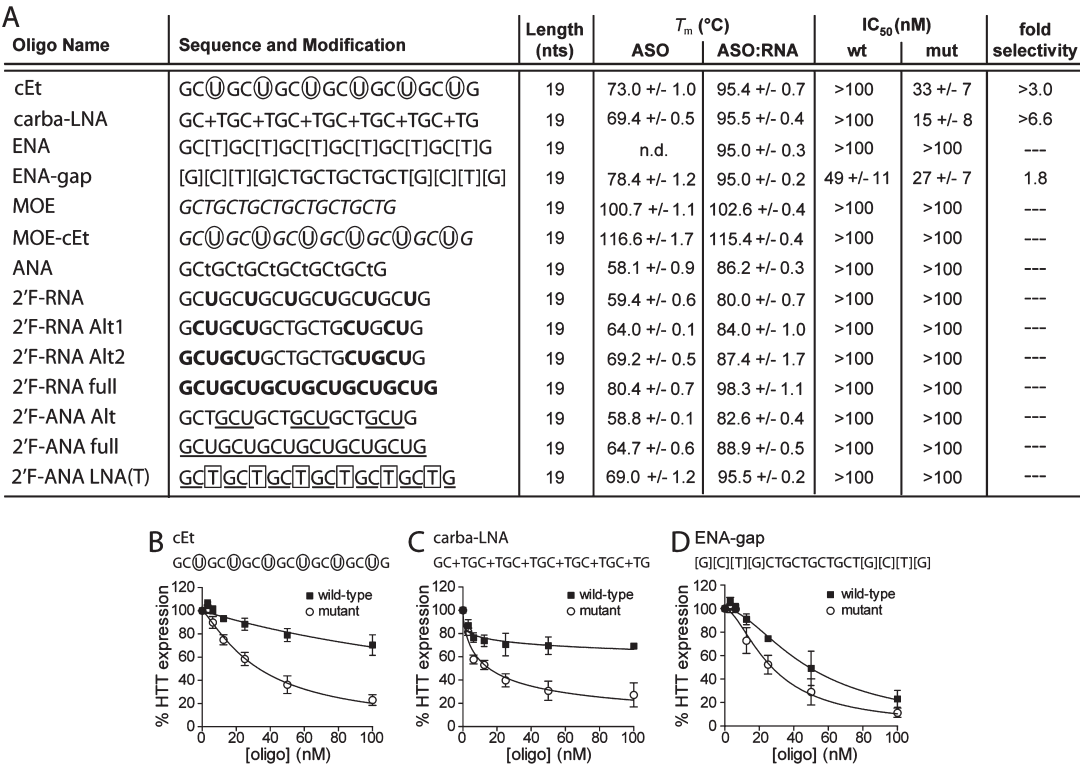
A

Oligo Name	Sequence and Modification	Length (nts)	T_m (°C) ASO	T_m (°C) ASO:RNA	IC_{50}(nM) wt	IC_{50}(nM) mut	fold selectivity
cEt	GCⓊGCⓊGCⓊGCⓊGCⓊGCⓊG	19	73.0 +/- 1.0	95.4 +/- 0.7	>100	33 +/- 7	>3.0
carba-LNA	GC+TGC+TGC+TGC+TGC+TGC+TG	19	69.4 +/- 0.5	95.5 +/- 0.4	>100	15 +/- 8	>6.6
ENA	GC[T]GC[T]GC[T]GC[T]GC[T]GC[T]G	19	n.d.	95.0 +/- 0.3	>100	>100	---
ENA-gap	[G][C][T][G]CTGCTGCTGCT[G][C][T][G]	19	78.4 +/- 1.2	95.0 +/- 0.2	49 +/- 11	27 +/- 7	1.8
MOE	*GCTGCTGCTGCTGCTGCTG*	19	100.7 +/- 1.1	102.6 +/- 0.4	>100	>100	---
MOE-cEt	*GCⓊGCⓊGCⓊGCⓊGCⓊG*	19	116.6 +/- 1.7	115.4 +/- 0.4	>100	>100	---
ANA	GCtGCtGCtGCtGCtGCtG	19	58.1 +/- 0.9	86.2 +/- 0.3	>100	>100	---
2'F-RNA	GC**U**GC**U**GC**U**GC**U**GC**U**G	19	59.4 +/- 0.6	80.0 +/- 0.7	>100	>100	---
2'F-RNA Alt1	GC**U**GC**U**GCTGCTG**C**UGC**U**G	19	64.0 +/- 0.1	84.0 +/- 1.0	>100	>100	---
2'F-RNA Alt2	**GCUGCU**GCTGCTG**CUGCU**G	19	69.2 +/- 0.5	87.4 +/- 1.7	>100	>100	---
2'F-RNA full	**GCUGCUGCUGCUGCUGCUG**	19	80.4 +/- 0.7	98.3 +/- 1.1	>100	>100	---
2'F-ANA Alt	GCT<u>GC</u>TGCT<u>GC</u>TGCT<u>GC</u>TG	19	58.8 +/- 0.1	82.6 +/- 0.4	>100	>100	---
2'F-ANA full	<u>GCTGCTGCTGCTGCTGCTG</u>	19	64.7 +/- 0.6	88.9 +/- 0.5	>100	>100	---
2'F-ANA LNA(T)	<u>GC</u>Ⓣ<u>GC</u>Ⓣ<u>GC</u>Ⓣ<u>GC</u>Ⓣ<u>GC</u>Ⓣ<u>G</u>	19	69.0 +/- 1.2	95.5 +/- 0.2	>100	>100	---

FIGURE 3: The BNA modifications LNA, cEt, and carba-LNA support allele-selective *HTT* inhibition. (A) Properties of ASOs containing various modifications. ASO, antisense oligonucleotide alone; ASO:RNA, antisense oligonucleotide duplexed with complementary RNA. Position of nucleotide modifications within the ASO sequence are indicated as follows: boxed, LNA; circled, cEt; preceded by a "+", carba-LNA; bracketed, ENA; italicized, MOE; lowercase, ANA; bold, 2'F-RNA; underlined, 2'F-ANA. T_m values were experimentally determined by UV melt analysis for ASOs and differential scanning calorimetry (DSC) for ASO:RNA duplexes and the MOE and MOE-cEt ASOs. Error is standard deviation. IC_{50} values are calculated from Western blot quantification. Values are reported in mean ± standard error of the mean (SEM). nd, not determined due to insufficient cooperativity. (B−D) HTT protein expression in patient-derived fibroblast cells containing 69 CAG repeats in the mutant allele (GM04281) in response to increasing doses of inhibitory modified ASO. Quantification and a nonlinear fit of *HTT* expression levels from multiple dose responses are plotted. Sequence and modification configuration are indicated above the graph. Error bars are SEM.

MOE modifications (Figures 3, S2 and S5 of the Supporting Information).

Quantification of Western blots after dose−response treatment with cET and carba-LNA revealed > 3.0- and > 6.6-fold selectivity, respectively (Figure 3). The IC_{50} for carba-LNA was 15 nM, while the value for cET was 33 nM. The ENA-gap ASO inhibited expression of both alleles with poor selectivity and moderate toxicity (Figure S4 of the Supporting Information), a result similar to that achieved using the LNA-modified gapmer LNA-gap (Figure 2). The remaining modified ASOs did not yield substantial inhibition of either wild-type or mutant *HTT* expression (Figure S5 of the Supporting Information).

It is interesting that some modifications yielded potent allele-selective inhibitors, whereas others did not. Several of the ASOs showed reduced hybridization affinities for complementary RNA compared to BNA-modified oligonucleotides (Figure 2A and 3A), especially the ANA, 2'F-RNA, 2'F-ANA, and 2'-FANA full designs. Reduced affinity for the target sequence provides one simple explanation for lack of inhibition.

Other inactive ASOs, however, such as fully modified 2'F-RNA full and 2'F-ANA LNA(T), had T_m values that were similar to active ASOs. For example, inactive 2'F-ANA LNA(T) had a melting temperature comparable to LNA(T) but was not inhibitory. The 2'F-ANA modification is known to acquire a south/east pucker and prefer a B-form helix (66) and thus acquires more DNA-like properties but with less flexibility (67). These properties may disrupt a unique helical structure that is induced by periodically spaced BNA-modified oligonucleotides and required

for inhibition of *HTT* expression (68). Indeed, LNA influences adjacent nucleotides by inducing them into a northern conformation (42).

For the ENA ASO, which also showed poor cooperativity in UV melt analysis, flexibility and self-structure may play a role in its lack of inhibition. The modification is considered intrinsically more flexible due to a longer bridge and a greater rotation around its δ bond angle (48). The 2'-O-(2-methoxyethyl) modification (MOE) combined with cEt (MOE-cEt) resulted in similar T_m values for the ASO alone or in combination with RNA (Figure 3A), suggesting that oligonucleotide self-structure may be too stable and thus reduce productive hybridization with complementary RNA in the cell.

Another possible contribution to the differences observed between modifications is that, although all modified oligomers contain similar phosphodiester backbones, the ribose modifications may lead to different levels of cellular uptake when transfected with different transfection reagents. To investigate this possibility, we tested delivery of duplex RNA siHdh1 and the LNA(T), MOE, 2'-F-RNA full, and 2'-F-ANA full ASOs using the delivery agents Lipofectamine RNAiMAX (Invitrogen), TriFECTin (Integrated DNA Technologies, Inc.), *Trans*IT-Oligo (Mirus), Oligofectamine (Invitrogen), and PepMute (SignaGen), following the manufacturer's recommended protocols (Figure S6 of the Supporting Information).

We observed that several lipids yielded poor inhibition of *HTT* expression by LNA(T), demonstrating that the choice of lipid does affect whether activity is observed. By contrast, use of the
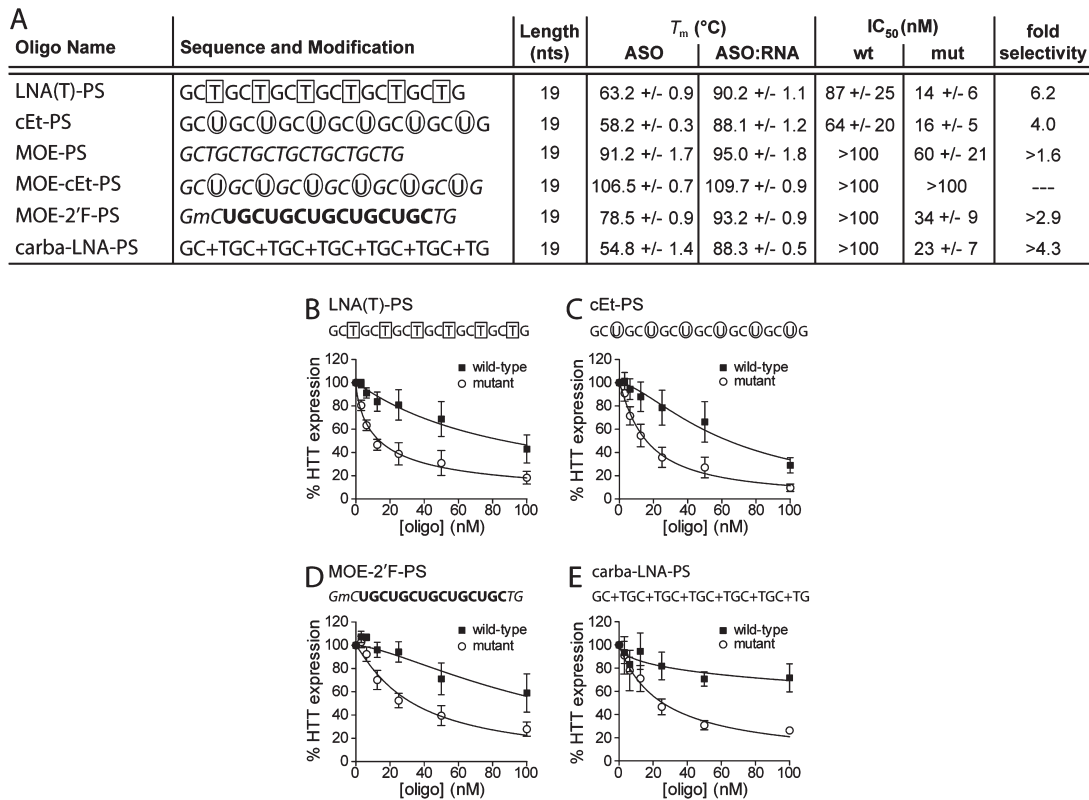
A

Oligo Name	Sequence and Modification	Length (nts)	T_m (°C) ASO	T_m (°C) ASO:RNA	IC_{50}(nM) wt	IC_{50}(nM) mut	fold selectivity
LNA(T)-PS	GC⊤GC⊤GC⊤GC⊤GC⊤G	19	63.2 +/- 0.9	90.2 +/- 1.1	87 +/- 25	14 +/- 6	6.2
cEt-PS	GCⓊGCⓊGCⓊGCⓊGCⓊG	19	58.2 +/- 0.3	88.1 +/- 1.2	64 +/- 20	16 +/- 5	4.0
MOE-PS	*GCTGCTGCTGCTGCTGCTG*	19	91.2 +/- 1.7	95.0 +/- 1.8	>100	60 +/- 21	>1.6
MOE-cEt-PS	*GCⓊGCⓊGCⓊGCⓊGCⓊG*	19	106.5 +/- 0.7	109.7 +/- 0.9	>100	>100	---
MOE-2′F-PS	*GmC***UGCUGCUGCUGCUGC***TG*	19	78.5 +/- 0.9	93.2 +/- 0.9	>100	34 +/- 9	>2.9
carba-LNA-PS	GC+TGC+TGC+TGC+TGC+TGC+TG	19	54.8 +/- 1.4	88.3 +/- 0.5	>100	23 +/- 7	>4.3

FIGURE 4: Phosphorothioate backbone modification is compatible with allele-selective inhibition. (A) Properties of CTG-repeat ASOs containing select modifications and a uniform phosphorothioate (PS) backbone. ASO, antisense oligonucleotide alone; ASO:RNA, antisense oligonucleotide duplexed with complementary RNA. Modification positions within the sequence are indicated as follows: boxed, LNA; circled, cET; italicized, MOE; bold, 2′F-RNA; preceded by a "+", carba-LNA; mC, 5-methyl cytosine. T_m values were experimentally determined by UV melt analysis for ASOs and differential scanning calorimetry (DSC) for ASO:RNA duplexes and the MOE-PS and MOE-cEt-PS ASOs. Error is standard deviation. IC_{50} values are calculated from Western blot quantification. Values are reported in mean ± standard error of the mean (SEM). (B−E) HTT protein expression in patient-derived fibroblast cells containing 69 CAG repeats in the mutant allele (GM04281) in response to increasing doses of inhibitory phosphorothioate-modified ASOs. Quantification and a nonlinear fit of *HTT* expression levels from multiple dose responses are plotted. Sequence and modification configuration are indicated above the graph. Error bars are SEM.

peptide-based delivery agent PepMute not only yielded efficient inhibition of *HTT* expression by LNA(T) but also showed that inhibition by MOE was also achievable. These data make the important general point that choice of transfection reagent can affect comparisons between oligomer chemistries. Results should be interpreted conservatively. Positive data indicates that inhibition of gene expression can be achieved and encourages further experimentation, but negative data can not always be assumed to indicate that an oligomer cannot function under any experimental conditions.

Effect of Phosphorothioate Substitution. Phosphorothioate (PS) modifications confer favorable pharmacological properties upon ASOs including increased stability against nuclease digestion and improved biodistribution (*38*). To determine whether introduction of PS linkages was compatible with allele-selective inhibition, we replaced all phosphodiester bonds in several oligonucleotides with the PS modification (Figure 4). Three of the ASOs, LNA(T)-PS, cEt-PS, and carba-LNA-PS, were based upon phosphodiester designs already shown to be allele-selective (Figures 2 and 3). One design was novel, MOE-2′F-PS, and combined two modifications, 2′F-RNA and MOE, not previously observed to yield allele-selective ASOs alone (Figure 3).

PS-substituted ASOs LNA(T)-PS, cEt-PS, MOE-2′F-PS, and carba-LNA-PS achieved potent and selective inhibition of *HTT* (Figure 4A). This inhibition was observed even though the four ASOs possessed reduced melting temperatures compared to analogous active ASOs that have phosphodiester linkages. MOE-PS and MOE-cEt-PS showed little selectivity, although they displayed mild inhibition (Figure S7 of the Supporting Information). MOE-PS and MOE-cEt-PS had similar melting temperatures for the ASO alone and the corresponding ASO: RNA duplex, suggesting highly stable self-structure. All phosphorothioate ASOs displayed some toxicity (Figure S4 of the Supporting Information). Although PS-modified oligonucleotides often show some level of toxicity in tissue culture cells, they are generally nontoxic when introduced into live animals at effective doses (*69−71*). These data demonstrate that allele-selective inhibition is compatible with the pharmacologically favorable PS modification.

Selective Inhibition in Cell Lines with Minimal CAG Repeats. The mean CAG repeat length in HD patients is 44 (*72*). Patient-derived fibroblasts containing 69 CAG repeats in the mutant allele and 17 in the normal allele (GM04281) were employed for initial studies because separation of the two proteins is relatively straightforward, facilitating the screening of numerous compounds. To determine whether ASOs would also selectively inhibit mutant *HTT* expression when CAG repeat length was more characteristic of most HD patients, we tested inhibition by the most promising compounds in GM04719 (44 mutant repeats/15 wild-type repeats) or GM04717 (41 mutant repeats/20 wild-type repeats) patient-derived fibroblasts.

LNA(T), cET, and carba-LNA were tested in both the 44 repeat and 41 repeat cell lines and achieved allele-selective
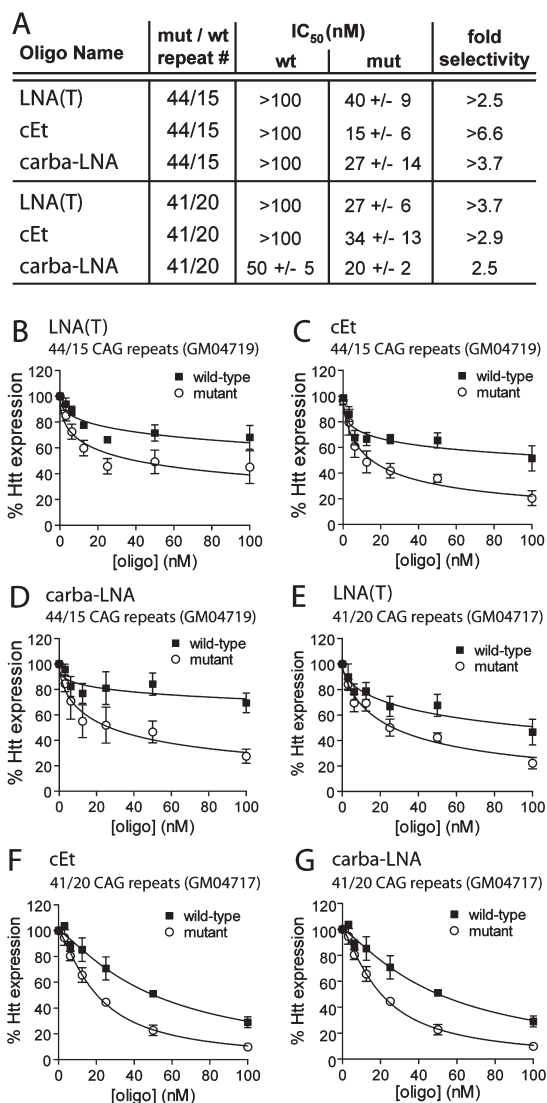
A

Oligo Name	mut / wt repeat #	IC$_{50}$ (nM) wt	mut	fold selectivity
LNA(T)	44/15	>100	40 +/- 9	>2.5
cEt	44/15	>100	15 +/- 6	>6.6
carba-LNA	44/15	>100	27 +/- 14	>3.7
LNA(T)	41/20	>100	27 +/- 6	>3.7
cEt	41/20	>100	34 +/- 13	>2.9
carba-LNA	41/20	50 +/- 5	20 +/- 2	2.5

B LNA(T) 44/15 CAG repeats (GM04719)

C cEt 44/15 CAG repeats (GM04719)

D carba-LNA 44/15 CAG repeats (GM04719)

E LNA(T) 41/20 CAG repeats (GM04717)

F cEt 41/20 CAG repeats (GM04717)

G carba-LNA 41/20 CAG repeats (GM04717)

FIGURE 5: Allele-selective ASOs discriminate between mutant and wild-type alleles in patient-derived fibroblasts with 44 or 41 CAG repeats in the mutant *HTT* mRNA. (A) Allele-selectivity and potency of three selective ASOs when targeting mutant *HTT* mRNAs with only 44 or 41 CAG repeats. IC$_{50}$ values are calculated from Western blot quantification. Values are reported in mean ± standard error of the mean (SEM). (B−G) HTT protein expression in patient-derived fibroblast cells containing 44 (GM04719) or 41 (GM04717) CAG repeats in the mutant allele in response to increasing doses of inhibitory ASOs. Quantification and a nonlinear fit of *HTT* expression levels from multiple dose responses are plotted. Error bars are SEM.

inhibition of *HTT* (Figure 5). IC$_{50}$ values for inhibition of mutant *HTT* ranged from 15 to 40 nM (Figure 5A−G and Figure S8 of the Suopporting Information). The allele-selectivity of inhibition varied between 2.5-fold to >6.6-fold. These data demonstrate that selectivity can be achieved in cell lines with mutant *HTT* alleles containing relatively few repeats.

Specificity for the Expanded CAG Repeat HTT Allele. Other human genes also have tracts of CAG repeats, although these tracts are usually much shorter than those observed for mutant *HTT* mRNA (*62*). A major concern for using ASO's to selectively block mutant *HTT* expression would be off-target inhibition of other genes. We have previously shown that peptide−PNA conjugates and the benchmark ASO LNA(T) do not affect endogenous CAG-repeat gene expression (*33*). To evaluate the potential for off-target effects with allele-selective ASOs composed of various chemical modifications, we treated

patient-derived GM04281 fibroblasts and monitored expression of repeat-containing genes. Western blot analysis showed no effect for these ASOs on the expression levels of TATA-box binding protein (TBP), which harbors CAG repeat tracts of up to 19 repeats in the coding region, or forkhead box protein p2 (FOXP2), which contains a mixed stretch of 40 CAG and CAA repeats in the 5′-UTR (Figure S9 of the Supporting Information). Ultimately, the possibility of toxicity due to off-target effects must be tested in vivo, but our experiments suggest that there is a window for achieving specific inhibition of mutant HTT. Efficient inhibition by ASOs may require CAG repeat expansions beyond a certain threshold length and perhaps also be dependent on the context of the surrounding sequence.

The Effect of Allele-Selective ASOs on HTT mRNA Levels and RNase H Activity. Antisense oligonucleotides targeted to mRNA typically inhibit gene expression by inducing degradation or blocking translation (*38, 57, 69*). To investigate the mechanism of allele-selective ASOs, we examined their effect on levels of *HTT* mRNA (Figure 6A). As a positive control, we demonstrated that transfection with 25 nM of siHdh1, a duplex RNA complementary to *HTT* mRNA at a sequence downstream of the CAG repeat (*63*), reduced total *HTT* mRNA levels to <20%. Treatment with a scrambled LNA control, (−) CTL, and a variety of allele-selective ASOs at 50 nM had little affect on *HTT* mRNA levels. Thus, RNA degradation does not appear to be a major determinant of allele-selective *HTT* inhibition.

We also tested the ability of allele-selective ASOs to support RNase H activity in vitro (Figure 6B). The 5′-end of mutant *HTT* mRNA containing 69 CAG repeats flanked by nonrepetitive sequences was cloned as cDNA from GM04281 cells and in vitro transcribed (Figure S10 of the Supporting Information). The resultant REP69 RNA was 5′-radiolabeled, hybridized to ASO, and treated with RNase H. The noncomplementary (−)CTL oligonucleotide had no effect on RNA stability. As expected, the DNA22 and LNA-gap yielded efficient cleavage. Cleavage of the RNA substrate was not readily detectable when RNase H was added in combination with the allele-selective LNA(T), cEt-PS, and MOE-2′F-PS oligonucleotides. These results are consistent with the conclusion that allele-selective ASOs targeting the expanded *HTT* CAG repeat may function through a steric translational block mechanism rather than RNase H activity.

Properties of an Allele-Selective ASO. Allele-selective ASOs exhibit high melting temperatures both alone and when hybridized with complementary RNA (Figures 1A, 2A, and 3A). To better characterize the properties of allele-selective ASOs, we monitored melting of the benchmark antisense oligonucleotide LNA(T), either alone or annealed to fully complementary RNA. In the absence of its RNA partner, LNA(T) alone melted with two clear transitions (Figure 7A). T_m values for each transition were not dependent on concentration of LNA(T) (Figure 7B), indicating that the observed transitions were due to intramolecular structure formation. These intramolecular structures are most likely hairpins. Thermal denaturation of the LNA(T):RNA duplex using DSC revealed a very stable complex with a single unfolding transition and a T_m of ∼97 °C (Figure 7C). These observations point to the conclusion that LNA(T) can form stable intramolecular interactions but that the interactions do not interfere with the formation of a stable duplex with complementary RNA.

Cumulative Binding of Multiple ASOs as a Mechanism for Allele-Selectivity. Mutant *HTT* repeats have more sites for
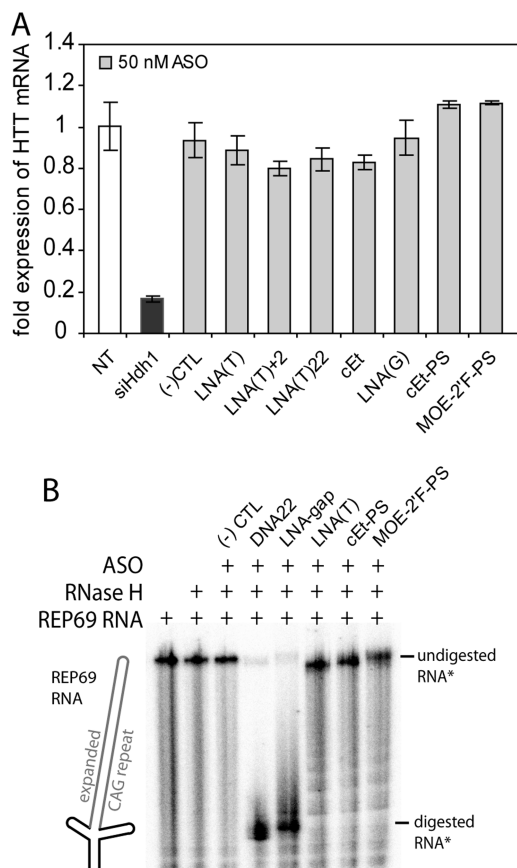
FIGURE 6: Allele-selective ASOs leave *HTT* mRNA intact and do not support RNase H activity in vitro. (A) *HTT* mRNA levels are not substantially affected by treatment with allele-selective ASOs as determined by quantitative RT-PCR. Amplification of *HTT* cDNA was normalized to GAPDH amplification. NT, nontransfected. siHdh1 (transfected at 25 nM) is a duplex siRNA targeted to sequence downstream of the *HTT* CAG repeat (*63*). Error bars are standard deviation of triplicate experiments. (B) Allele-selective ASOs do not support RNase H cleavage in vitro. Allele-selective ASOs or control oligonucleotides were incubated with an in vitro transcribed and 5'-radiolabeled 69 CAG repeat-containing *HTT* mRNA 5' end transcripts followed by treatment with RNase H enzyme. Reaction products were resolved on a denaturing polyacrylamide gel then visualized by a phosphorimager.
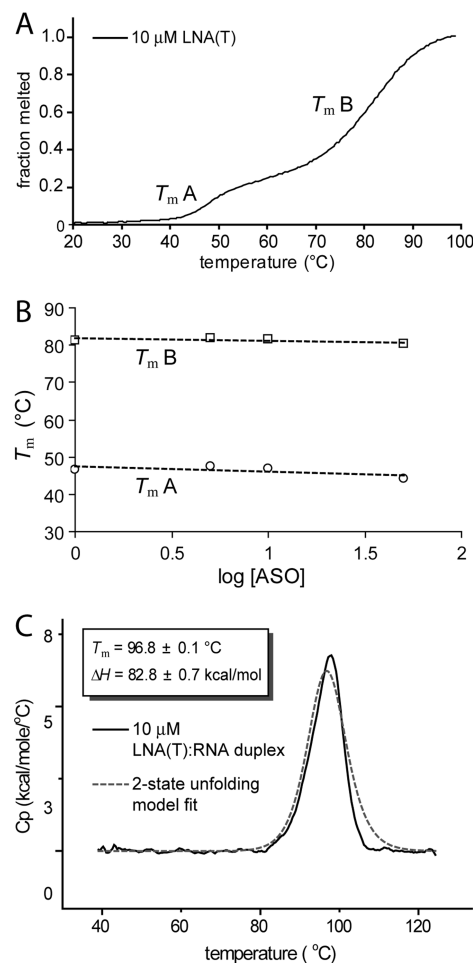

FIGURE 7: The allele-selective ASO LNA(T) forms a stable self-structure and RNA:ASO duplex. (A) UV melt analysis of LNA(T), an allele-selective inhibitor of *HTT* expression, in the absence of an RNA complement. (B) UV melts of LNA(T) at concentrations spanning almost 2 orders of magnitude show no concentration dependence for T_m, suggesting an intramolecular hairpin folded structure. T_m (A) and T_m (B) correspond to the indicated transitions in panel A. (C) Differential scanning calorimetry (DSC) of LNA(T) base-paired to a fully complementary RNA. The ASO:RNA duplex is exceptionally stable, with a T_m of ~97 °C. Values were fit to a two-state unfolding model to calculate ΔH at the T_m.

ASO binding than do wild-type repeats. For example, a 69 CAG repeat sequence can bind up to ten 20-base ASOs, whereas a 17-base wild-type repeat sequence can bind no more than two to three. Therefore, one simple mechanism that might contribute to selective inhibition would be binding of more ASOs to the mutant repeat than to the wild-type.

We performed in vitro binding assays to gain insights into the varying levels of allele-selectivity elicited by ASOs (Figure 8). Complementary DNA (cDNA) of mRNA 5'-ends from mutant and normal *HTT* mRNA were cloned from GM04281 cells and in vitro transcribed. Both RNAs begin at the start codon and continue past the CAG repeat. The cloned region was designed to incorporate flanking RNA sequence to preserve any surrounding mRNA structure that might be critical to native folding of the repeat (Figure S10 of the Supporting Information).

Mutant RNA (REP69) and normal RNA (REP17) were 5'-radiolabeled, refolded, and mixed with increasing concentrations of ASO followed by resolution of ASO:RNA complexes on native polyacrylamide gels. The different ASOs appeared to bind with varying affinities. Interestingly, the MOE-cEt ASO did not

bind REP69 and only poorly bound REP17 RNA. Because this oligonucleotide exhibited such stable self-structure (Figure 3A), it may be unable to overcome kinetic or thermodynamic barriers to bind the target RNA.

Binding by multiple oligomers could be observed for most ASOs. Discrete bands corresponding to individual binding events were observed over the course of the titration. This resulted in 10 or more ASOs hybridizing to the REP69 RNA and between 2 and 3 ASOs for the REP17 RNA, both near upper limits of binding events predicted considering ASO and target CAG repeat lengths. These findings suggest that the quantity of ASOs able to bind a folded *HTT* mRNA in vitro are only limited by the number of CAG repeats available, consistent with the CAG repeat being a semistable but accessible hairpin structure (*58, 59, 73*). Quantification of gels followed by fitting to a Hill equation revealed strong sigmoidal curves and Hill coefficients around 2, indicative of cooperative ASO binding (Figure 8C and S11 of the Supporting Information). While the situation inside cells is not known, these data from in vitro assays suggest that cumulative and cooperative binding of ASOs to longer mutant CAG repeats
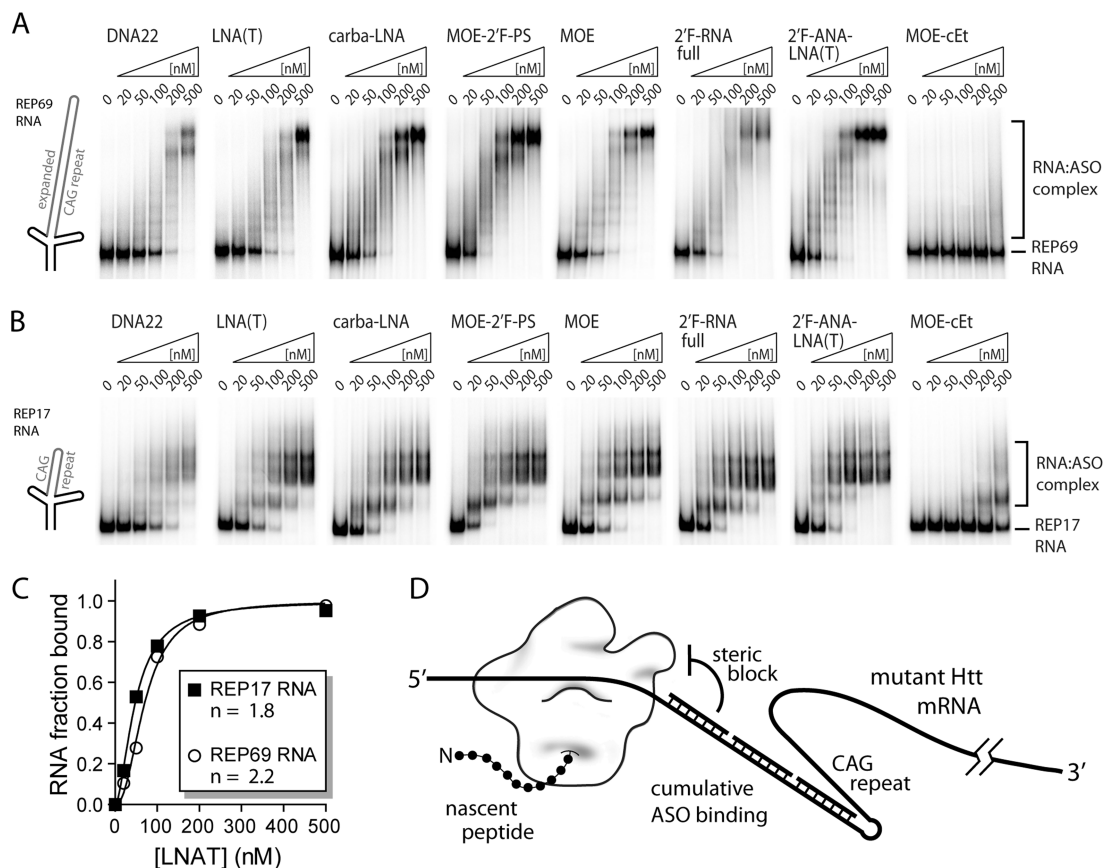
FIGURE 8: Multiple ASOs bind CAG repeat-containing *HTT* 5′-end transcripts in vitro. (A−B) Electrophoretic mobility shift assays (EMSA) demonstrate cooperative and near stoichiometric binding of multiple ASOs to CAG repeat sequence in *HTT* mRNA 5′ end transcripts, as well as a case where no binding is observed. In vitro transcribed and 5′-radiolabeled wild-type and mutant 5′-end *HTT* mRNA transcripts were incubated with increasing concentrations of ASO. RNA:ASO complexes were resolved on native polyacrylamide gels and visualized by phosphorimager. ASO concentrations are indicated above the gels and shifted bands identified to the right. (C) Quantification of LNA(T) binding REP17 and REP69 *HTT* mRNA transcripts indicates cooperative ASO binding. ASO-bound RNA in gel shifts from (A) and (B) were quantified and plotted as a function of concentration. Fitting to the Hill equation revealed a sigmoidal binding curve and Hill coefficients (*n*) near 2, suggesting cooperative ASO binding. (D) Putative steric translational blocking mechanism. Translation is repressed on a mutant expanded CAG repeat *HTT* mRNA due to a proposed steric inhibition of translation by cumulative ASO binding.

may contribute to increased recognition and allele-selectivity (Figure 8D).

DISCUSSION

Development of safe and effective strategies for reducing expression of *HTT* is an important goal for HD research. siRNAs or ASOs offer nucleic acid based strategies for achieving this goal. While nucleic acids are not a traditional approach toward development of therapies for brain disorders, recent advances in their chemistry, pharmacology, and delivery have made them a realistic option for diseases like HD where patients have no curative treatments available (*74, 75*).

It is possible that useful siRNAs or ASOs will be effective even if they cause equal reduction of both *HTT* alleles (*25*). However, given the potential unknown side effects of long-term inhibition of normal *HTT* expression in patients with HD, allele-selective strategies offer a useful addition to the treatment options being considered (*26*). Allele-selective siRNAs that exploit single nucleotide polymorphisms for specificity are the subject of intense interest by several laboratories (*28, 30−32*).

While siRNAs and antisense oligonucleotides inhibit gene expression through similar mechanisms, they have different strengths. siRNAs benefit from an endogenous gene regulatory pathway, RNA interference (RNAi), and are incorporated into the RNA-induced silencing complex (RISC) to guide degrada-

tion of complementary RNA. These properties can make siRNAs robust inhibitors of gene expression and help protect them from degradation (*76*).

ASOs offer an alternate approach. Because they are single-stranded, they can be less expensive to manufacture. They do not need to be incorporated into a protein complex, possibly leading to more predictable off-target effects and the potential for more extensive chemical modification (*69*). ASOs have been thoroughly tested in the clinic and may prove to be a more direct route to a nucleic acid based therapeutic for allele-specific inhibition of mutant *HTT* expression (*26, 37−41*). ASOs, by virtue of being half the size of duplex RNAs, may show better distribution in vivo, although this possibility has not yet been demonstrated. Pursuing both the ASO and siRNA strategies should maximize the likelihood that a useful agent will eventually benefit HD patients.

We have identified 10 chemically modified ASOs that selectively inhibited expression of the mutant *HTT* allele. A number of chemical modifications to the ribose were compatible with allele-selective inhibition, including LNA, cEt, carba-LNA, MOE, and 2′F-RNA, and phosphodiester internucleotide linkages could be substituted with phosphorothioate. When three ASOs were tested in patient-derived cell lines containing fewer CAG repeats that are more representative of the HD patient population, they all showed allele-selective inhibition. At least five ASOs of diverse

chemistry appeared specific for the expanded CAG repeat of *HTT* because they had no effect on two unrelated genes containing substantial CAG repeat tracts. Although tentative, design rules for allele-selective ASOs targeting expanded CAG repeats should include high hybridization affinity tempered with moderate intramolecular self-structure. Among the allele-selective ASOs, bridged nucleic acids were highly successful and should be considered as lead modifications.

It is not always straightforward to understand why some ASOs are more effective than others, especially with such a wide variety of modification types and configurations under evaluation. A number of factors can complicate an oligonucleotide's ability to reach its target RNA and inhibit gene expression. Simple explanations might include poor transfection or release from endosomes after cell entry. Future studies will be needed to more clearly determine why some chemical modifications were ineffective and why even among the bridged nucleic acid modifications there were varying degrees of inhibition and selectivity. Nonetheless, our data provide a broad choice of compounds for testing in vivo or for further optimization as drug candidates.

Our data suggest that allele-selective inhibition can be achieved by a mechanism involving a steric block of translation (Figure 8D). The most successful allele-selective ASOs did not have the central DNA bases found in gapmer antisense oligonucleotides and did not support RNase H activity in vitro. Allele-selective ASOs also had little or no effect on *HTT* mRNA levels. We previously reported that a fully complementary CTG:CAG repeat small duplex RNA (siREP) targeted to the CAG repeat, which presumably induces RNA cleavage in the *HTT* repeat region via the RNA-induced silencing complex (RISC), was a robust inhibitor of *HTT* expression but very nonselective (*33, 34*). Taken together, these results suggest that directed cleavage of RNA does not contribute significantly to the mechanism of allele-selective inhibition.

In support of a translational inhibition model for allele-selectivity, our ASOs bound CAG repeat RNA in a cooperative manner in vitro, with multiple ASOs assembling onto all of the potentially available CAG repeat sequence. Thus, selective inhibition could arise from greater accumulation of ASOs on the expanded CAG repeat *HTT* mRNA and preferentially block translation of the mutant HTT protein. Cooperative binding could also contribute to the specificity of allele-selective ASOs for the *HTT* mRNA by enhancing affinity with each binding event as the RNA structure is invaded and becomes increasingly more accessible. Investigations of the CAG repeat structure for other mRNAs suggests that *HTT* mRNA may well have unique properties that help facilitate cooperative ASO binding (*59, 73*). In addition, effective translational repression by ASOs is often achieved when targeting near the start codon of an mRNA (*45, 77*). The expanded CAG repeat of *HTT* is near the 5′-end of the mRNA, with only 51 nucleotides between the translational start site and the beginning of the CAG repeat tract, making it a good candidate for translational repression by antisense oligonucleotides.

Our findings suggest that targeting repeats may serve as a general strategy for developing nucleic acid based therapeutics for disease-related genes that harbor simple repeat expansions. A recent report demonstrated the therapeutic potential of a CAG-repeat morpholino targeted to DM protein kinase (DMPK) mRNA, which contains a CUG repeat expansion in myotonic dystrophy type 1 (DM1) (*36*). The morpholino disrupted ribonucleoprotein complexes formed between the expanded CUG repeat of DMPK mRNA and muscleblind-like 1 (MBNL-1) protein, an interaction directly implicated in disease. Competition with the complementary morpholino released MBNL-1 and rescued the myotonic dystrophy phenotype in a mouse model of DM. Most trinucleotide and some tetranucleotide repeat expansions form semistable hairpin structures, much like that observed in the CAG repeat region of *HTT* (*58, 59, 73*). Thus, simple repeat sequences should be generally amenable to targeting with complementary ASOs to selectively modulate gene expression and ultimately provide new hope for currently untreatable genetic diseases.

ACKNOWLEDGMENT

SUPPORTING INFORMATION AVAILABLE

Derivation of experimental T_m values from UV melt analysis and DSC, representative Western blots for quantification of *HTT* inhibition with allele-selective or control ASOs or ASOs that showed poor inhibition or selectivity in patient derived cells with 69 CAG repeats in the mutant allele, viability of patient-derived fibroblasts after treatment with various ASOs, inhibition of *HTT* expression with several ASOs using different transfection reagents, representative Western blots for quantification of *HTT* inhibition in patient-derived cells with 44 or 41 CAG repeats, Western blots showing specificity of allele-selective ASOs for the mutant *HTT* gene, sequence and predicted secondary structure of the 5′-end of *HTT* mRNA transcripts, and quantification of multiple ASOs that appear to cooperatively bind REP17 and REP69 *HTT* RNA transcripts. This material is available free of charge via the Internet at http://pubs.acs.org.

REFERENCES

1. Orr, H. T., and Zoghbi, H. Y. (2007) Trinucleotide repeat disorders. *Annu. Rev. Neurosci. 30*, 575–621.
2. Walker, F. O. (2007) Huntington's disease. *Lancet 369*, 218–228.
3. MacDonald, M. E., Ambrose, C. M., Duyao, M. P., Myers, R. H., Lin, C., Srinidhi, L., Barnes, G., Taylor, S. A., James, M., Groot, N., and MacFarlane, H.; et al. (1993) A novel gene containing a trinucleotide repeat that is expanded and unstable on Huntington's disease chromosomes. *Cell 72*, 971–983.
4. Rubinsztein, D. C. (2003) Molecular biology of Huntington's disease (HD) and HD-like disorders., in Genetics of Movement Disorders (Pulst, S., Ed.), pp 365−377, California Academic Press, Millbrae CA.
5. Rubinsztein, D. C., Leggo, J., Coles, R., Almqvist, E., Biancalana, V., Cassiman, J. J., Chotai, K., Connarty, M., Crauford, D., and Curtis, A.; et al. (1996) Phenotypic characterization of individuals with 30−40 CAG repeats in the Huntington disease (HD) gene reveals HD cases with 36 repeats and apparently normal elderly individuals with 36−39 repeats. *Am. J. Hum. Genet. 59*, 16–22.
6. McNeil, S. M., Novelletto, A., Srinidhi, J., Barnes, G., Kornbluth, I., Altherr, M. R., Wasmuth, J. J., Gusella, J. F., MacDonald, M. E., and Myers, R. H. (1997) Reduced penetrance of the Huntington's disease mutation. *Hum. Mol. Genet. 6*, 775–779.
7. Kremer, B., Goldberg, P., Andrew, S. E., Theilmann, J., Telenius, H., Zeisler, J., Squitieri, F., Lin, B., Bassett, A., Almqvist, E., Bird, T. D., and Hayden, M. R. (1994) A worldwide study of the Huntington's disease mutation. The sensitivity and specificity of measuring CAG repeats. *N. Engl. J. Med. 330*, 1401–1406.
8. Snell, R. G., MacMillan, J. C., Cheadle, J. P., Fenton, I., Lazarou, L. P., Davies, P., MacDonald, M. E., Gusella, J. F., Harper, P. S., and Shaw, D. J. (1993) Relationship between trinucleotide repeat expansion and phenotypic variation in Huntington's disease. *Nature Genet. 4*, 393–397.

9. Rangone, H., Humbert, S., and Saudou, F. (2004) Huntington's disease: how does huntingtin, an anti-apoptotic protein, become toxic? *Pathol. Biol. 52*, 338–342.

10. Luo, G. R., and Le, W. D. (2010) Collective roles of molecular chaperones in protein degradation pathways associated with neurodegenerative diseases. *Curr. Pharm. Biotechnol. 11*, 180–187.

11. Ross, C. A., and Poirier, M. A. (2004) Protein aggregation and neurodegenerative disease. *Nature Med. 10*, S10–S17.

12. Hayden, M. R., Leavitt, B. R., Yasothan, U., and Kirkpatrick, P. (2009) Tetrabenazine. *Nature Rev. Drug Discovery 8*, 17–18.

13. Stewart, J. T. (1988) Treatment of Huntington's disease with clonazepam. *South Med. J. 81*, 102.

14. Grote, H. E., Bull, N. D., Howard, M. L., van Dellen, A., Blakemore, C., Bartlett, P. F., and Hannan, A. J. (2005) Cognitive disorders and neurogenesis deficits in Huntington's disease mice are rescued by fluoxetine. *Eur. J. Neurosci. 22*, 2081–2088.

15. Peng, Q., Masuda, N., Jiang, M., Li, Q., Zhao, M., Ross, C. A., and Duan, W. (2008) The antidepressant sertraline improves the phenotype, promotes neurogenesis and increases BDNF levels in the R6/2 Huntington's disease mouse model. *Exp. Neurol. 210*, 154–163.

16. Goehler, H., Lalowski, M., Stelzl, U., Waelter, S., Stroedicke, M., Worm, U., Droege, A., Lindenberg, K. S., Knoblich, M., and Haenig, C.; et al. (2004) A protein interaction network links GIT1, an enhancer of huntingtin aggregation, to Huntington's disease. *Mol. Cell 15*, 853–865.

17. Bae, B. I., Xu, H., Igarashi, S., Fujimuro, M., Agrawal, N., Taya, Y., Hayward, S. D., Moran, T. H., Montell, C., and Ross, C. A.; et al. (2005) p53 mediates cellular dysfunction and behavioral abnormalities in Huntington's disease. *Neuron 47*, 29–41.

18. DiProspero, N. A., Chen, E. Y., Charles, V., Plomann, M., Kordower, J. H., and Tagle, D. A. (2004) Early changes in Huntington's disease patient brains involve alterations in cytoskeletal and synaptic elements. *J. Neurocytol. 33*, 517–533.

19. Charrin, B. C., Saudou, F., and Humbert, S. (2005) Axonal transport failure in neurodegenerative disorders: the case of Huntington's disease. *Pathol. Biol. 53*, 189–192.

20. Bauer, P. O., and Nukina, N. (2009) The pathogenic mechanisms of polyglutamine diseases and current therapeutic strategies. *J. Neurochem. 110*, 1737–1765.

21. Gagnon, K. T. (2010) HD Therapeutics—CHDI Fifth Annual Conference, *IDrugs 13*, 219–223.

22. Nasir, J., Floresco, S. B., O'Kusky, J. R., Diewert, V. M., Richman, J. M., Zeisler, J., Borowski, A., Marth, J. D., Phillips, A. G., and Hayden, M. R. (1995) Targeted disruption of the Huntington's disease gene results in embryonic lethality and behavioral and morphological changes in heterozygotes. *Cell 81*, 811–823.

23. White, J. K., Auerbach, W., Duyao, M. P., Vonsattel, J. P., Gusella, J. F., Joyner, A. L., and MacDonald, M. E. (1997) *Huntingtin* is required for neurogenesis and is not impaired by the Huntington's disease CAG expansion. *Nature Genet. 17*, 404–410.

24. Duyao, M. P., Auerbach, A. B., Ryan, A., Persichetti, F., Barnes, G. T., McNeil, S. M., Ge, P., Vonsattel, J. P., Gusella, J. F., and Joyner, A. L.; et al. (1995) Inactivation of the mouse Huntington's disease gene homolog *Hdh*. *Science 269*, 407–410.

25. Drouet, V., Perrin, V., Hassig, R., Dufour, N., Auregan, G., Alves, S., Bonvento, G., Brouillet, E., Luthi-Carter, R., Hantraye, P., and Déglon, N. (2009) Sustained effects of nonallele-specific *Huntingtin* silencing. *Ann. Neurol. 65*, 276–285.

26. Scholefield, J., and Wood, M. J. (2010) Therapeutic gene silencing strategies for polyglutamine disorders. *Trends Genet. 26*, 29–38.

27. Miller, V. M., Xia, H., Marrs, G. L., Gouvion, C. M., Lee, G., Davidson, B. L., and Paulson, H. L. (2003) Allele-specific silencing of dominant disease genes. *Proc. Natl. Acad. Sci. U.S.A. 100*, 7195–7200.

28. van Bilsen, P. H., Jaspers, L., Lombardi, M. S., Odekerken, J. C., Burright, E. N., and Kaemmerer, W. F. (2008) Identification and allele-specific silencing of the mutant huntingtin allele in Huntington's disease patient-derived fibroblasts. *Hum. Gene Ther. 19*, 710–718.

29. Rodriguez-Lebron, E., and Paulson, H. L. (2006) Allele-specific RNA interference for neurological disease. *Gene Ther. 13*, 576–581.

30. Zhang, Y., Engelman, J., and Friedlander, R. M. (2009) Allele-specific silencing of mutant Huntington's disease gene. *J. Neurochem. 108*, 82–90.

31. Pfister, E. L., Kennington, L., Straubhaar, J., Wagh, S., Liu, W., DiFiglia, M., Landwehrmeyer, B., Vonsattel, J. P., Zamore, P. D., and Aronin, N. (2009) Five siRNAs targeting three SNPs may provide therapy for three-quarters of Huntington's disease patients. *Curr. Biol. 19*, 774–778.

32. Lombardi, M. S., Jaspers, L., Spronkmans, C., Gellera, C., Taroni, F., Di Maria, E., Donato, S. D., and Kaemmerer, W. F. (2009) A majority of Huntington's disease patients may be treatable by individualized allele-specific RNA interference. *Exp. Neurol. 217*, 312–319.

33. Hu, J., Matsui, M., Gagnon, K. T., Schwartz, J. C., Gabillet, S., Arar, K., Wu, J., Bezprozvanny, I., and Corey, D. R. (2009) Allele-specific silencing of mutant huntingtin and ataxin-3 genes by targeting expanded CAG repeats in mRNAs. *Nature Biotechnol. 27*, 478–484.

34. Hu, J., Matsui, M., and Corey, D. R. (2009) Allele-selective inhibition of mutant huntingtin by peptide nucleic acid-peptide conjugates, locked nucleic acid, and small interfering RNA. *Ann. N.Y. Acad. Sci. 1175*, 24–31.

35. Hu, J., Dodd, D. W., Hudson, R. H., and Corey, D. R. (2009) Cellular localization and allele-selective inhibition of mutant huntingtin protein by peptide nucleic acid oligomers containing the fluorescent nucleobase [bis-*o*-(aminoethoxy)phenyl]pyrrolocytosine. *Bioorg. Med. Chem. Lett. 19*, 6181–6184.

36. Wheeler, T. M., Sobczak, K., Lueck, J. D., Osborne, R. J., Lin, X., Dirksen, R. T., and Thornton, C. A. (2009) Reversal of RNA dominance by displacement of protein sequestered on triplet repeat RNA. *Science 325*, 336–339.

37. Corey, D. R. (2007) Chemical modification: the key to clinical application of RNA interference? *J. Clin. Invest. 117*, 3615–3622.

38. Swayze, E. E., Bhat, B. (2008) The Medicinal Chemistry of Oligonucleotides, in Antisense Drug Technology: Principles, Strategies, and Applications (Crooke, S. T., Ed.) 2nd ed., pp 143–182, CRC Press, Boca Raton, FL.

39. Raal, F. J., Santos, R. D., Blom, D. J., Marais, A. D., Charng, M. J., Cromwell, W. C., Lachmann, R. H., Gaudet, D., Tan, J. L., and Chasan-Taber, S.; et al. (2010) Mipomersen, an apolipoprotein B synthesis inhibitor, for lowering of LDL cholesterol concentrations in patients with homozygous familial hypercholesterolaemia: a randomised, double-blind, placebo-controlled trial. *Lancet 375*, 998–1006.

40. Akdim, F., Visser, M. E., Tribble, D. L., Baker, B. F., Stroes, E. S., Yu, R., Flaim, J. D., Su, J., Stein, E. A., and Kastelein, J. J. (2010) Effect of mipomersen, an apolipoprotein B synthesis inhibitor, on low-density lipoprotein cholesterol in patients with familial hypercholesterolemia. *Am. J. Cardiol. 105*, 1413–1419.

41. Akdim, F., Stroes, E. S., Sijbrands, E. J., Tribble, D. L., Trip, M. D., Jukema, J. W., Flaim, J. D., Su, J., Yu, R., and Baker, B. F.; et al. (2010) Efficacy and safety of mipomersen, an antisense inhibitor of apolipoprotein B, in hypercholesterolemic subjects receiving stable statin therapy. *J. Am. Coll. Cardiol. 55*, 1611–1618.

42. You, Y., Moreira, B. G., Behlke, M. A., and Owczarzy, R. (2006) Design of LNA probes that improve mismatch discrimination. *Nucleic Acids Res. 34*, e60.

43. Obika, S., Nanbu, D., Hari, Y., Andoh, J., Morio, K., Doi, T., and Imanishi, T. (1998) Stability and structural features of the duplexes containing nucleoside analogues with a fixed N-type conformation, 2′-*O*,4′-*C*-methyleneribonucleosides. *Tetrahedron Lett. 39*, 5401–5404.

44. Koshkin, A. A., Singh, S. K., Nielsen, P., Rajwanshi, V. K., Kumar, R., Meldgaard, M., Olsen, C. E., and Wengel, J. (1998) LNA (Locked Nucleic Acids): Synthesis of the adenine, cytosine, guanine, 5-methylcytosine, thymine and uracil bicyclonucleoside monomers, oligomerisation, and unprecedented nucleic acid recognition. *Tetrahedron 54*, 3607–3630.

45. Braasch, D. A., Liu, Y., and Corey, D. R. (2002) Antisense inhibition of gene expression in cells by oligonucleotides incorporating locked nucleic acids: effect of mRNA target sequence and chimera design. *Nucleic Acids Res. 30*, 5160–5167.

46. Kaur, H., Arora, A., Wengel, J., Maiti, S., Arora, A., Wengel, J., and Maiti, S. (2006) Thermodynamic, Counterion, and Hydration Effects for the Incorporation of Locked Nucleic Acid Nucleotides into DNA Duplexes. *Biochemistry 45*, 7347–7355.

47. Morita, K., Hasegawa, C., Kaneko, M., Tsutsumi, S., Sone, J., Ishikawa, T., Imanishi, T., and Koizumi, M. (2002) 2′-*O*,4′-*C*-ethylene-bridged nucleic acids (ENA): highly nuclease-resistant and thermodynamically stable oligonucleotides for antisense drug. *Bioorg. Med. Chem. Lett. 12*, 73–76.

48. Koizumi, M., Morita, K., Daigo, M., Tsutsumi, S., Abe, K., Obika, S., and Imanishi, T. (2003) Triplex formation with 2′-*O*,4′-*C*-ethylene-bridged nucleic acids (ENA) having C3′-endo conformation at physiological pH. *Nucleic Acids Res. 31*, 3267–3273.

49. Seth, P. P., Siwkowski, A., Allerson, C. R., Vasquez, G., Lee, S., Prakash, T. P., Wancewicz, E. V., Witchell, D., and Swayze, E. E. (2009) Short antisense oligonucleotides with novel 2′-4′ conformationaly restricted nucleoside analogues show improved potency without increased toxicity in animals. *J. Med. Chem. 52*, 10–13.

50. Prakash, T. P., Siwkowski, A., Allerson, C. R., Migawa, M. T., Lee, S., Gaus, H. J., Black, C., Seth, P. P., Swayze, E. E., and Bhat, B. (2010) Antisense oligonucleotides containing conformationally constrained 2′,4′-(*N*-methoxy)aminomethylene and 2′,4′-aminooxymethylene and 2′-*O*,4′-*C*-aminomethylene bridged nucleoside analogues show improved potency in animal models. *J. Med. Chem.* 53, 1636–1650.

51. Srivastava, P., Barman, J., Pathmasiri, W., Plashkevych, O., Wenska, M., and Chattopadhyaya, J. (2007) Five- and six-membered conformationally locked 2′,4′-carbocyclic ribo-thymidines: synthesis, structure, and biochemical studies. *J. Am. Chem. Soc.* 129, 8362–8379.

52. Allart, B., Khan, K., Helmut, R., Schepers, G., Hendrix, C., Rothenbacher, K., Seela, F., Van Aerschot, A., and Herdewijn, P. (1999) D-Altritol nucleic acids (ANA): hybridisation properties, stability, and initital structural analysis. *Chem.—Eur. J.* 5, 2424–2431.

53. Teplova, M., Minasov, G., Tereshko, V., Inamati, G. B., Cook, P. D., Manoharan, M., and Egli, M. (1999) Crystal structure and improved antisense properties of 2′-*O*-(2-methoxyethyl)-RNA. *Nature Struct. Biol.* 6, 535–539.

54. Kawasaki, A. M., Casper, M. D., Freier, S. M., Lesnik, E. A., Zounes, M. C., Cummins, L. L., Gonzalez, C., and Cook, P. D. (1993) Uniformly modified 2′-deoxy-2′-fluoro phosphorothioate oligonucleotides as nuclease-resistant antisense compounds with high affinity and specificity for RNA targets. *J. Med. Chem.* 36, 831–841.

55. Watts, J. K., and Damha, M. J. (2008) 2′F-Arabinonucleic acids (2′F-ANA)—History, properties, and new frontiers. *Can. J. Chem.* 86, 641–656.

56. Damha, M. J., Wilds, C. J., Noronha, A., Brukner, I., Borkow, G., Arion, D., and Parniak, M. A. (1998) Hybrids of RNA and arabinonucleic acids (ANA and 2′F-ANA) are substrates of ribonuclease H. *J. Am. Chem. Soc.* 120, 12976–12977.

57. Bonham, M. A., Brown, S., Boyd, A. L., Brown, P. H., Bruckenstein, D. A., Hanvey, J. C., Thomson, S. A., Pipe, A., Hassman, F., and Bisi, J. E.; et al. (1995) An assessment of the antisense properties of RNase H-competent and steric-blocking oligomers. *Nucleic Acids Res.* 23, 1197–1203.

58. Broda, M., Kierzek, E., Gdaniec, Z., Kulinski, T., and Kierzek, R. (2005) Thermodynamic stability of RNA structures formed by CNG trinucleotide repeats. Implication for prediction of RNA structure. *Biochemistry* 44, 10873–10882.

59. Sobczak, K., Michlewski, G., de Mezer, M., Kierzek, E., Krol, J., Olejniczak, M., Kierzek, R., and Krzyzosiak, W. J. (2010) Structural diversity of triplet repeat RNAs. *J. Biol. Chem.* 285, 12755–12764.

60. Chakrabarti, M. C., and Schwarz, F. P. (1999) Thermal stability of PNA/DNA and DNA/DNA duplexes by differential scanning calorimetry. *Nucleic Acids Res.* 27, 4801–4806.

61. Kaur, H., Wengel, J., and Maiti, S. (2008) Thermodynamics of DNA−RNA heteroduplex formation: effects of locked nucleic acid nucleotides incorporated into the DNA strand. *Biochemistry* 47, 1218–1227.

62. Kozlowski, P., de Mezer, M., and Krzyzosiak, W. J. (2010) Trinucleotide repeats in human genome and exome. *Nucleic Acids Res.* 38, 4027–4039.

63. Omi, K., Hachiya, N. S., Tokunaga, K., and Kaneko, K. (2005) siRNA-mediated inhibition of endogenous Huntington disease gene expression induces an aberrant configuration of the ER network in vitro. *Biochem. Biophys. Res. Commun.* 338, 1229–1235.

64. Brion, P., Michel, F., Schroeder, R., and Westhof, E. (1999) Analysis of the cooperative thermal unfolding of the *td* intron of bacteriophage T4. *Nucleic Acids Res.* 27, 2494–2502.

65. Mergny, J.-L., and Lacroix, L. (2003) Analysis of thermal melting curves. *Oligonucleotides* 13, 515–537.

66. Ikeda, H., Fernandez, R., Wilk, A., Barchi, J. J., Jr., Huang, X., and Marquez, V. E. (1998) The effect of two antipodal fluorine-induced sugar puckers on the conformation and stability of the Dickerson−Drew dodecamer duplex [d(CGCGAATTCGCG)]2. *Nucleic Acids Res.* 26, 2237–2244.

67. Mangos, M. M., Min, K.-L., Viazovkina, E., Galarneau, A., Elzagheid, M. I., Parniak, M. A., and Damha, M. J. (2002) Efficient RNase H-directed cleavage of RNA promoted by antisense DNA or 2′F-ANA constructs containing acyclic nucleotide inserts. *J. Am. Chem. Soc.* 125, 654–661.

68. Kaur, H., Wengel, J., and Maiti, S. (2007) LNA-modified oligonucleotides effectively drive intramolecular-stable hairpin to intermolecular-duplex state. *Biochem. Biophys. Res. Commun.* 352, 118–122.

69. Crooke, S. T. (2004) Progress in antisense technology. *Annu. Rev. Med.* 55, 61–95.

70. Henry, S. P., Templin, M. V., Gillett, N., Rojko, J., and Levin, A. A. (1999) Correlation of Toxicity and Pharmacokinetic Properties of a Phosphorothioate Oligonucleotide Designed to Inhibit ICAM-1. *Toxicol. Pathol.* 27, 95–100.

71. Ferdinandi, E. S., Vassilakos, A., Lee, Y., Lightfoot, J., Fitsialos, D., Wright, J. A., Young, A. H. (2010) Preclinical toxicity and toxicokinetics of GTI-2040, a phosphorothioate oligonucleotide targeting ribonucleotide reductase R2, *Cancer Chemother. Pharmacol.* 66, doi: 10.1007/s00280-010-1473-z.

72. Andrew, S. E., Goldberg, Y. P., Kremer, B., Telenius, H., Theilmann, J., Adam, S., Starr, E., Squitieri, F., Lin, B., and Kalchman, M. A.; et al. (1993) The relationship between trinucleotide (CAG) repeat length and clinical features of Huntington′s disease. *Nature Genet.* 4, 398–403.

73. Michlewski, G., and Krzyzosiak, W. J. (2004) Molecular architecture of CAG repeats in human disease related transcripts. *J. Mol. Biol.* 340, 665–679.

74. Hua, Y., Sahashi, K., Hung, G., Rigo, F., Passini, M. A., Bennett, C. F., and Krainer, A. R. (2010) Antisense correction of SMN2 splicing in the CNS rescues necrosis in a type III SMA mouse model. *Genes Dev.* 24, 1634–1644.

75. Smith, R. A., Miller, T. M., Yamanaka, K., Monia, B. P., Condon, T. P., Hung, G, Lobsinger, C. S., Ward, C. M., McAlonis-Downes, M., and Wei, H.; et al. (2006) Antisense oligonucleotide therapy for neurodegenerative disease. *J. Clin. Invest.* 116, 2290–2296.

76. Watts, J. K., Deleavey, G. F., and Damha, M. J. (2008) Chemically modified siRNA: tools and applications. *Drug Discovery Today* 13, 842–855.

77. Dias, N., Dheur, S., Nielsen, P. E., Gryaznov, S., Van Aerschot, A., Herdewijn, P., Helene, C., and Saison-Behmoaras, T. E. (1999) Antisense PNA tridecamers targeted to the coding region of Ha-ras mRNA arrest polypeptide chain elongation. *J. Mol. Biol.* 294, 403–416.